ACS Photonics

Article

pubs.acs.org/journal/apchd5

Interfacial Organization in Dipolar Dye-Based Organic Nanoparticles Probed by Second-Harmonic Scattering

Jonathan Daniel, Flavie Bondu, Frédéric Adamietz, Mireille Blanchard-Desce, and Vincent Rodriguez*

Institut des Sciences Moléculaires, CNRS UMR5255, Université de Bordeaux, 351 Cours de la Libération, 33405 Talence Cedex, France

ABSTRACT: We have undertaken polarization-resolved SHS experiments to investigate a series of two fluorescent organic nanoparticles (FONs) made from dipolar dyes bearing a triphenylamine-donating end-group and a slightly hydrophilic acceptor end-group. The FONs, which show very large negative surface potentials, responsible for their good colloidal stability in water, are very bright SHS emitters in water, attractive for single-particle tracking and bioimaging. With the polarization-resolved SHS technique, we come up with a new and noninvasive method to gain insight into the origin of the surface potential of the FONs, as well as into their evolution upon change of ionic strength by following their multipolar response when adding salt. In pure water, the polarization-resolved SHS spectroscopy reveals the presence of a region of local polar order close to the surface (i.e., orientation of the dipolar dyes), leading to a strong dipolar contribution. Quite interestingly, when adding KCl salt, the initial two-lobe SHS polar plot transforms into a four-lobe pattern with a net decrease of the SHS intensity, revealing a lower surface potential. Second, we have quantified the decrease of the SHS signal when adding salt with the goal to estimate the change of the NPs' colloidal stability in salty media. From a simple equilibrium model that we propose, we have extracted a lower bound free energy for the two FONs, which are thermally accessible and in good accordance with their respective colloidal stability.

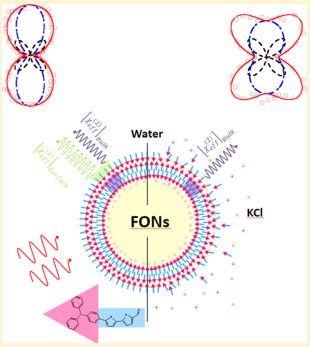

KEYWORDS: *second-harmonic scattering, fluorescent organic nanoparticles, dipolar chromophores, colloidal stability*

In the last decades, nanoparticles have attracted increased interest in biology and optoelectronics fields, mainly due to their unique properties. Among them, luminescent metal- and semiconductor-based nanoparticles have attracted overwhelming attention. A number of them however raise toxicity and biodegradability issues, which is critical with regard to biomedical applications and environmental concerns. In that perspective, molecular-based fluorescent organic nanoparticles (FONs)[1] emerged as a promising alternative toward optical nanomaterials and fluorescent probes for acute biomaging applications.[2] Among them, FONs made from specific dyes, i.e., dipolar (i.e., push−pull or D−π−A compound) chromophores, offer attractive features as tunable luminescent nanomaterials[3] of interest for cellular as well as *in vivo* bioimaging purposes[4] or as nanotools for single-particle tracking.[5] Interestingly, the colloidal stability of these nanoparticles in water was observed to strongly depend on the structure of the push−pull compound system.[4,6] Furthermore, investigation of the fluorescence properties (in particular fluorescence emission spectra and lifetimes) reveals different environments, pointing to possible nanostructuration of dipolar dyes within the FONs. Conjecturing that this could be ascribed to a specific organization (and local ordering) of the dye subunits near the surface of the spherically shaped FONs (i.e., at the interface with water), we aimed at investigating this hypothesis by using hyper-Rayleigh scattering (HRS), also called harmonic light scattering (HLS) or second-harmonic scattering (SHS). Indeed HRS is a powerful selective method for characterizing molecules,[7,8] aggregates,[9] and dispersed nanoparticles (NPs) in liquids.[10,11] However, note that HRS (or equivalently HLS) is appropriate in the case of molecular scattering whether SHS is the more general term that is actually adapted for nanoparticle scattering since the latter are sizable particles. Highly dispersed NPs behave identically with molecules in the sense that each NP or molecule is an individual electric dipole emitter; i.e., they are incoherent sources of scattered light where no phase relation occurs between emitters. However, one expects a nonlocal electric dipole response for each NP due to the finite nanoscale size. This means that the SHS response of an NP includes additional interference terms with possible retardation effects. Note that electric quadrupolar contribution may also occur. However, in the electric dipole response a bulk centrosymmetric media is not SHS active. On the contrary, any interface is SHS active since there is a symmetry breaking at the interface. This makes SHS a very powerful interface-selective method to investigate structure, equilibrium, and time-dependent properties of interfaces.[10]

Herein we thus report the polarization-resolved SHS experiments that we have undertaken to investigate a series of FONs made from dipolar chromophores bearing a triphenylamine-donating end-group and a slightly hydrophilic acceptor end-group. The goal of the study was to examine the nature of the water/nanoparticle interface and determine specific chromophore organization near the surface. Both

Received: June 2, 2015
Published: July 15, 2015

DOI: 10.1021/acsphotonics.5b00301
ACS Photonics 2015, 2, 1209−1216

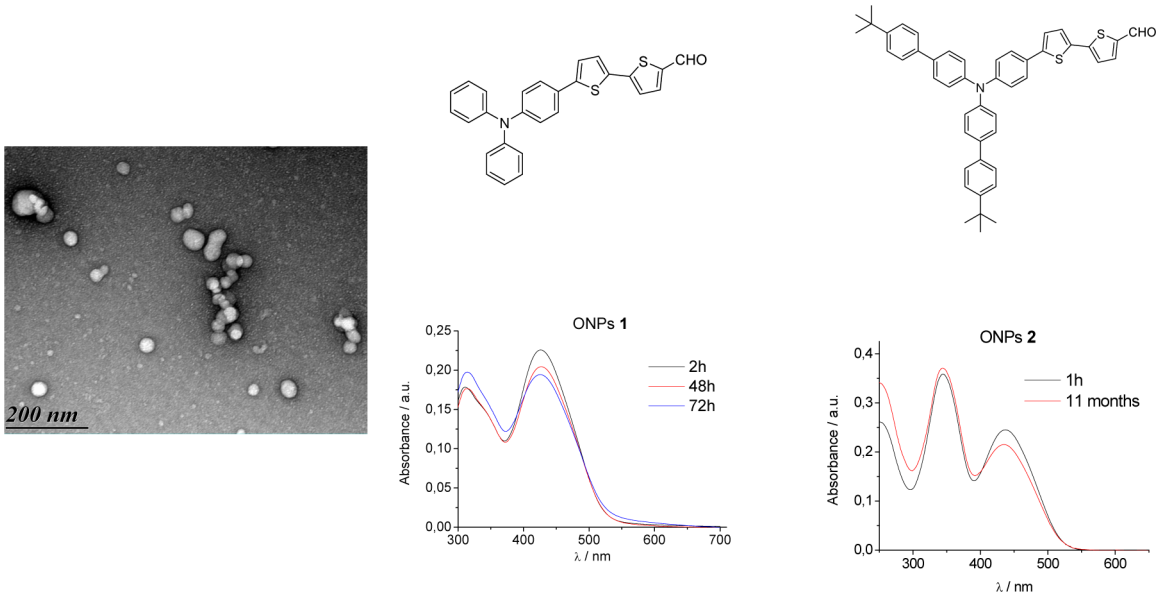

Figure 1. Left: TEM image of freshly prepared FONs made from precipitation of **2** in water. Middle and right: Evolution over time of the absorption spectra of FONs made from dyes **1** and **2** in water.

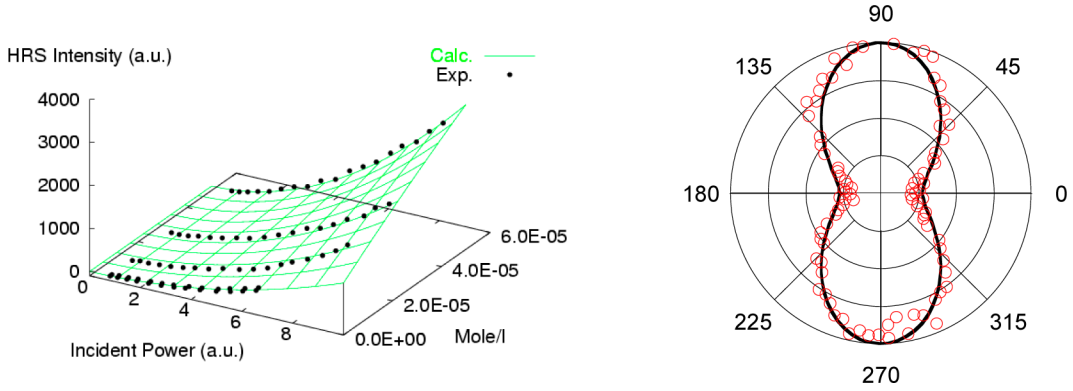

Figure 2. HRS responses of dye **1** in chloroform: 3D representation as a function of the incident power and concentration (left) and extracted polar plot of the polarization curve of the solvated dye (right). Circles are experimental data, and solid lines are best fitted curves according to equations (left) E1 and (right) E2, respectively.

dipolar chromophores **1**[6] and **2**[5] spontaneously give FONs upon reprecipitation in pure water. Whereas FONs made from dipolar dye **1** are stable over hours, those made from dipolar dye **2** are stable over days (Figure 1).

RESULTS AND DISCUSSION

Molecular Response in Organic Solution. A typical 3D representation of the hyper-Rayleigh scattering response of dipolar dye **1** dissolved in chloroform is reported in Figure 2. It nicely reports the linear relationship of the HRS response with the dye concentration as well as the quadratic dependence of the collected signal upon the incident power following eq E1 (see the Molecular Incoherent HRS Characterizations section). The polar plot of the polarization curve of the solvated dye following eq E2 exhibits two lobes with maxima for the VV (see the Molecular Incoherent HRS Characterizations section) configuration (Figure 2), although the octupolar response is slightly stronger than the dipolar one (see Table 1). The extracted data for dye **1** solvated in chloroform given in Table 1 are typical of a charge transfer chromophore where the absorption band (λ_{max} = 431 nm) occurs far enough from the harmonic response at 532 nm. The HRS response given by β_{HRS} is rather modest in comparison with prototypical dyes; for example, its amplitude is about 5 times lower than the prototypical octupolar crystal violet.[12]

Table 1. Molecular Data Deduced from HRS Measurements at 1064 nm[a]

	1 in $HCCl_3$	**1** in acetonitrile	**2** in $HCCl_3$
$\lvert\beta\rvert^2$ C_{VV}^{Incoh}	124×10^6	145×10^6	172×10^6
β_{HRS}	12.5×10^3	13.3×10^3	14.6×10^3
DR	3.6	4.6	4.1
ρ	1.22 ± 0.03	0.91 ± 0.03	1.05 ± 0.05
$\beta_{J=1}$	20.7×10^3	24.2×10^3	25.6×10^3
$\beta_{J=3}$	25.3×10^3	22.0×10^3	26.9×10^3

[a]Hyperpolarizabilities (with relative accuracy ca. 5%) are expressed in atomic units using convention T.[13] 1 atomic unit of $\beta = 3.62 \times 10^{-42}$ m^4 V^{-1} = 8.641×10^{-33} esu.

The results reported in Table 1 for dye **1** in acetonitrile indicate a nice solvatochromism effect as the dipolar character of the dye becomes the dominant multipolar contribution. As a consequence β_{HRS} of dye **1** in acetonitrile is ca. 6% higher than

DOI: 10.1021/acsphotonics.5b00301
ACS Photonics 2015, 2, 1209−1216

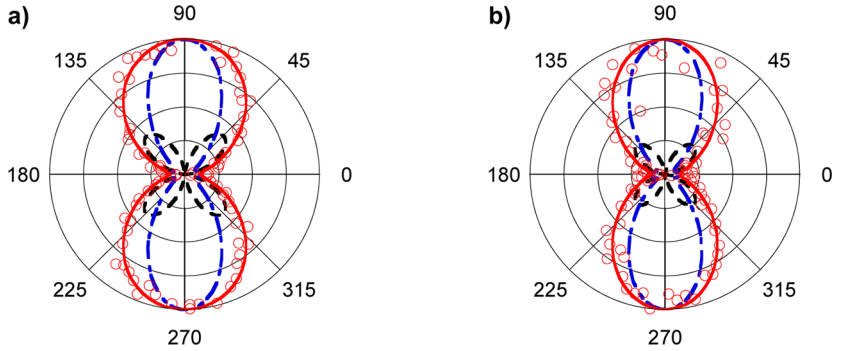

Figure 3. (a) Extracted SHS polar plot of solvated NPs **1** (a) and **2** (b), where circles are experimental data and red solid lines are best fits to eq E5. Blue and black dashed lines are the electric dipolar and quadrupolar contributions, respectively, according to eq E7.

in chloroform. Table 1 reports also HRS data of dye **2** in chloroform. Again the octupolar component is a little bit stronger than the dipolar one, and the whole response β_{HRS} of **2** is ∼15% stronger than that of **1** in chloroform, indicating that the two biphenyl arms modify only slightly the electronic feature and induce just a slight increase of the strength of the electron donating, resulting in a parallel slight red-shift of the low-energy absorption band (λ_{max} = 438 nm). To summarize, these two dyes are relatively good HRS emitters, exhibiting a 1D−2D charge transfer.

Second-Harmonic Scattering of Nanoparticles in Water. The surface charge density σ and the associated potential ϕ_0 are important characteristics of interfaces. They affect notably the structural arrangements of ionic and neutral species and also the stability of colloidal suspensions. The total SHS signal radiated by an NP includes two contributions. The first one comes from the interface and can be composed of two contributions, as detailed in eq 1.

$$[\beta]_{NP} = [\beta + \{\gamma\phi_0\}_{EFISH}]_{Interface} + [\beta]_{Bulk} \quad (1)$$

One is structural and comes from the second-order susceptibility (β) that originates from chemical species at the interface, i.e., here mainly triphenylamine-based dipolar chromophores. A polar H-aggregate arrangement at the water interface is indeed expected for dipolar chromophores where the hydrophobic triphenylamine end-group points toward the center of the NP while the somewhat hydrophilic formyl end-group points toward water. In addition the resulting interfacial potential ϕ_0 is also expected to trigger the formation of H-aggregate domains and potentially expand their spatial correlation in such a way that this net dipolar structural interfacial contribution may be very strong even if it is probably composed of inhomogeneous surface-oriented domains. The second interfacial contribution is a Kerr contribution called electric field induced second harmonic (EFISH), which involves the third-order susceptibility (γ) of the chromophores (which is strong for such two-photon absorbing dyes) and the interfacial potential ϕ_0. Note that both the chemical species at the interface and the water molecules in the bulk solution close to the surface are partially aligned by the electric field of the charged interface and contribute thus to the net EFISH response, as demonstrated by Eisenthal.[10] These bulk solution contributions are indeed relatively weak but are easily detected using femtosecond laser sources.

The last contribution to the SHS signal reported in eq 1 is the bulk contribution from the NPs. In the case of noncentrosymmetric nanocrystals with a ferroelectric response like, for example, $BaTiO_3$,[14,15] the SHS bulk response may be huge, with β ranging around 10^{-24} esu (∼10^9 atomic unit). On the contrary, in the case of a centrosymmetric bulk arrangement, the dipolar response cancels and only the remaining quadrupolar response can be detected.

For comparison purposes, poly(lactic-*co*-glycolic acid) (PLGA) NPs with a diameter (∼40 nm) and zeta potential (−70 mV) comparable to those of NPs **1** and **2** have been investigated. Since we expect a weak β molecular response for PLGA, no bulk contribution and no structural dipolar interfacial contribution are expected. However, despite a weak expected γ molecular response for PLGA, these NPs exhibit an interfacial EFISH contribution from PLGA and water molecules in the bulk solution close to the surface. Despite this, a SHS polar plot of PLGA NPs in water/THF (1%) (∼10^{-9} M) could not be detected, indicating thus that our experimental SHS setup, where a picosecond excitation laser line is used (see the Experimental and Theoretical Section for details), is not able to detect such a weak expected EFISH signal. Hence we clearly demonstrate with PLGA that we are unable with our setup to detect these very weak signals; that is, we are able to detect only high β and γ molecular chemical species (such as **1** and **2**).

Figure 3a and b report respectively the extracted SHS polar plot of solvated NPs **1** and **2** in water/THF (1%), and Table 2 gathers the different parameters obtained from that study following the procedure detailed in the section SHS Investigation of the Nanoparticles. Polar plots exhibit both two-lobe-polarized patterns, which are typical of a dominant electric dipolar response, as already observed for gold and silver NPs.[16]

Table 2. NP Data Deduced from SHS Measurements at 1064 nm[a]

in water/THF (1%)	1	2
$\lvert\beta\rvert^2$ C_{VV}^{Coh}	120 × 10^{12}	38 × 10^{12}
$\lvert\beta\rvert$	3.7 × 10^6	2.5 × 10^6
DR	8.7 ± 0.9	9.2 ± 1.8
Δ^{Coh}	12.4 ± 1.5	9.0 ± 2.3
Δ^{Q}	14.1 ± 0.5	11.2 ± 4.1
D_{NP}[b]	36	40
ζ[c]	−45	−75

[a]β components (with relative accuracy ca. 10%) are expressed in atomic units using convention T.[13] 1 atomic unit of β = 3.62 × 10^{-42} m^4 V^{-1} = 8.641 × 10^{-33} esu. [b]Diameter of the NP in nm. [c]Zeta potential of the NP in mV.

DOI: 10.1021/acsphotonics.5b00301
ACS Photonics 2015, 2, 1209−1216

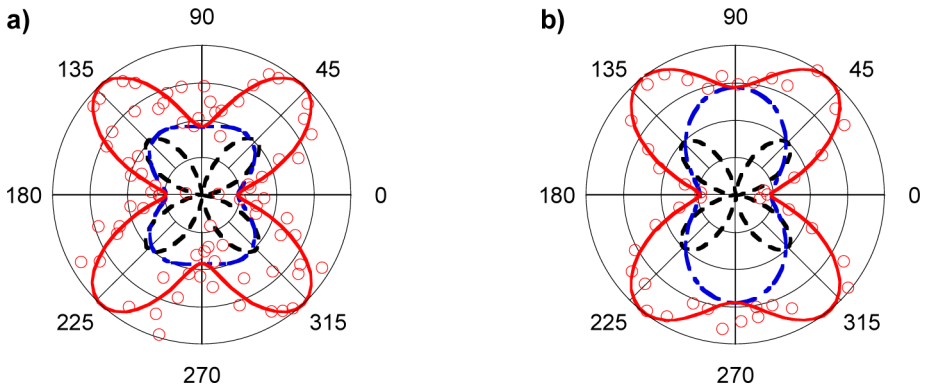

Figure 4. Extracted SHS polar plot of solvated NPs **1** (a) and **2** (b) in water/THF (1%)/0.2 M KCl. Circles are experimental data, and red solid lines are best fits to eq E5. Blue and black dashed lines are the electric dipolar and quadrupolar contributions, respectively, according to eq E7.

Comparing Table 2 and Table 1 SHS intensities (first lines), we immediately see that both NPs are one million times brighter than their respective molecular component. The NPs' hyperpolarizabilities $|\beta|$ are in the range of 10^6 atomic unit ($\sim 10^{-27}$ esu), which is typically 3 orders of magnitude lower than those of $BaTiO_3$ or $PbTiO_3$ ferroelectric nanocrystals with comparable diameters.[14] This large difference of response is a good indication that the *bulk* contribution of NPs **1** or **2** is probably very weak or zero. This point is in very good accordance with the centrosymmetric single-crystal packing of **1** (triclinic space group $P\bar{1}$).[6] Note however as a second point that the hyperpolarizability of NPs **1** is the greater one despite the molecular response of **1** remaining the smaller one. Since the NPs' sizes are comparable, we think that structural interfacial differences (and possibly bulk differences) may occur due to the presence of two additional *tert*-butylphenyl bulky side groups of **2**, which affects the polar order close to the NPs' surface (i.e., larger tilt angles of dipoles). Focusing now on the nature of the responses through the analyses of polarization scans following eq E5 (SHS Investigation of the Nanoparticles section), we observe that for both NPs the depolarization ratio (DR) is equal to 9 within the experimental error (Table 2). This indicates that the electric dipolar response exhibits no octupolar hyperpolarizability component and could be interpreted by the presence of highly correlated polar H-aggregate domains. The amount of polar domains is very important and probably covers a large part of the surface and/or the bulk of NPs since the dipolar response exceeds greatly the quadrupolar one, as illustrated in Figure 3. In principle, the quadrupolar contribution represented in Figure 3 and quantified by Δ^Q (Table 2) would come from the bulk response since it contains the larger amount of molecules. A detailed comprehensive analysis of these interfacial and bulk contributions is thus necessary to better understand the structure of these FONs.

How Does the Multipolar SHS Response of FONs Change When Adding an Electrolyte? Chemical species adopting a polar ordered structure at the interface with water are strongly perturbed by increasing the ionic strength of the solution, which modifies the surface potential.[17] It is well established that electrolytes can act to perturb the initial organization. The SHS responses of NPs **1** and **2** when adding KCl have thus been monitored. Figure 4 gives a typical extracted SHS polar plot of solvated NPs **1** and **2** in water with 0.2 M KCl. The addition of salt in the mixture is first characterized by a more or less pronounced decrease of the SHS signal depending on the NPs' composition. In addition, we observe now for both NPs four-lobe polarized patterns, which have been already observed for example in centrosymmetric micelles[18] or gold nanorods.[11] When comparing NPs **1** from Figures 3a and 4a, we clearly evidence a collapse of the dipolar β component against the octupolar one inside the electric dipolar response (blue dashed lines) when adding salt. Note that the quadrupolar response (four-lobe feature with maxima at 45° *modulo* 90°) remains similar with or without salt, indicating effectively that it is mostly a core bulk contribution. The trends are basically the same for NPs **2**; however we nicely observe that the collapse of the dipolar response is less pronounced, indicating that the stability of that colloid is really improved by the presence of bulky additional side groups of the dipolar chromophores (as already suggested by the larger surface potential).

As discussed in the literature, local electric dipolar contributions have been evidenced but from imperfect spherical gold or silver NPs. However, in the case of organic NPs, that type of local dipolar contribution is likely thought of as a statistical number of polar domains (i.e., H-type aggregates) that are highly structurally time correlated. These correlated domains made of elementary dipolar dyes are supposed to be ferroelectric (polar) domains at the interface with water because of the effect of the electric surface potential. Because of the relative small size of the NPs (diameter 40 nm), we hypothesize no retardation effects from the surface response. However, this may not be valid any longer when considering correlated domains inside the NP since we expect a dramatic increase of multiscattering processes, which produces retardation effects. Therefore, contributions from the bulk are thought to be in any case quadrupolar effective ones. They are either nonlocal electric dipole contributions if the bulk is structurally inhomogeneous, which means not totally centrosymmetric, or local electric quadrupolar contributions if the bulk is structurally centrosymmetric. We think that the reprecipitation method used to prepare FONs favors partial disorder since it is a nonequilibrium process (as opposed to slow crystallization) and thus produces mainly nonlocal electric dipole contributions.

Evolution of the Structure and Stability of FONs with Salt: Keys for Molecular Engineering. Here we aim to go a little further in the description of the structure and more interestingly in the stability of the FONs in the presence of electrolytes. The question of the colloidal stability of FONs in salty media is crucial for *in vivo* bioimaging applications.[4,6] For

DOI: 10.1021/acsphotonics.5b00301
ACS Photonics 2015, 2, 1209−1216

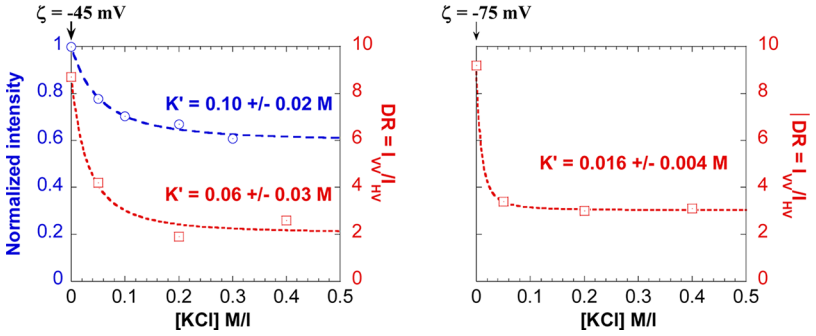

Figure 5. Evolution of extracted SHS data of solvated NPs **1** (left) and **2** (right) with KCl addition. Blue circles are experimental normalized SHS intensity data, and lines are best fits to eq 6. Red squares are experimental DR data, and dotted lines are best fits to eqs 6 and E6. The relative equilibrium constant K' (see text) obtained from each fit are reported.

that purpose we need to carefully analyze the modification of the SHS signal of NPs upon addition of salt and its variation as a function of the amount of added salt. Figure 5 reports the decrease of the normalized SHS intensity of NPs **1**, which reaches a plateau at around 0.2 M KCl, indicating thus that 40% of the intensity corresponding to the interface contribution has disappeared and 60% of the initial signal remains even at higher salt concentration, where the NP aggregation in microparticles increases strongly. As depicted in eq E6 (SHS Investigation of the Nanoparticles section), we observe also a very good correlation of the decrease of the depolarization ratio and the normalized SHS intensity when adding KCl. Since polarization scans contain the maximum of information that we can obtain with SHS measurement, we have also reported in Figure 5 the decrease of DR with salt for NPs **2**.

We observe that the decrease of the signal is very sharp for NPs **2**, indicating that there is quite an important difference in the interfacial structure evolution of NPs **2**, which exhibits better colloidal stability. With the SHS method, we come up with a new and noninvasive method to characterize the evolution and stability of the NPs. It is thus worth establishing a tentative quantitative description of that evolution.

This model assumes a modification of the distribution of molecules contributing to the surface SHS signal upon addition of salt. Starting from a polar site (PS) a molecule may either lose its polar orientation and switch to a nonpolar site (NPS) or be displaced to reach any other surface area to produce an empty polar site (EPS), which may partially destabilize the local polar ordering.

$$\begin{array}{cccc} \mathrm{PS} & \overset{[\mathrm{KCl}]}{\rightleftharpoons} & \mathrm{NPS} \quad \mathrm{EPS} & \\ N_{\max} & & 0 \quad 0 & t = 0 \\ N_{\max} - N & & xN \quad (1-x)N & t = \infty \end{array} \tag{2}$$

where $N_{\max}$ is the initial number of molecules in the polar sites contributing to the surface signal, N is the total number of molecules that lose their polar orientation, and x is the fraction number that details the balance between nonpolar or empty sites. At equilibrium we exclude *a priori* any possibility of dyes in the water bulk solution due to the insolubility of dyes **1** and **2** in water. The equilibrium constant K and its relation to the free energy of loss of polar response ΔG^0 is

$$K = \mathrm{e}^{-\Delta G^{\circ}/(RT)} = \frac{[\mathrm{NPS}][\mathrm{EPS}]}{[\mathrm{PS}]} = \frac{x(1-x)N^2}{N_{\max} - N} \tag{3}$$

Let us assume that the total number of molecules that lose their polar orientation N is proportional to the concentration of added salt $C = [\mathrm{KCl}]$ as

$$N = \alpha C \tag{4}$$

The equilibrium relative surface coverage of polar contributions yields

$$\frac{N}{N_{\max}} = \frac{1}{1 + C/K'} \tag{5}$$

where $K' = K/[\alpha x(1-x)]$ is the relative equilibrium constant.

The second-harmonic electric field from the surface is proportional to the density of polar molecules, which is proportional to the relative surface coverage of polar contributions $N/N_{\max}$, giving thus for the total SHS intensity

$$I_{\mathrm{VV}}^{2\omega} \propto [\beta]_{\mathrm{Np}}^2 = \left| \frac{[\beta + \{\gamma\phi_0\}_{\mathrm{EFISH}}]_{\mathrm{Interface}}}{(1 + C/K')} + [\beta]_{\mathrm{Bulk}} \right|^2 \tag{6}$$

Therefore, the relative equilibrium constant of the loss of surface polar contribution can be determined from the measured $N/N_{\max}$ and use of eq 6. Equivalently the experiment yields a lower bound of the corresponding free energy ΔG^0:

$$\Delta G^{\circ} = -RT \ln K' = -RT\{\ln K - \ln[\alpha x(1-x)]\} \tag{7}$$

We observe in Figure 5 that this model reproduces well both the total normalized SHS intensity and also DR. We obtain for NPs **1** a relative equilibrium constant $K' = 0.10 \pm 0.02$ M and $K' = 0.06 \pm 0.03$ M from the fit of the normalized intensity and the depolarization ratio, respectively. As expected, these two independently fitted values merge into a common range value within the experimental error. The corresponding lower bound free energy for NPs **1** at room temperature is $\Delta G^0 = +2.7$ kJ/M. As expected also, the obtained fitted value of the relative equilibrium constant of NPs **2** is ca. 1 order of magnitude lower, with $K' = (16 \pm 4) \times 10^{-3}$ M, giving a lower bound free energy at room temperature, $\Delta G^0 = +4.5$ kJ/M. The free energy is about 2 kJ/M less than NPs **1**, indicating quantitatively that NPs **2** are more stable colloids. In both cases the loss of polarity of the interface is not a spontaneous process since the free energy is positive but the lower bound value is easily thermally accessible ($RT = +2.5$ kJ/M).

The different behavior of NPs **1** and **2** clearly points to the importance of the structure of the dipolar dyes that constitute the NPs in controlling the organization at the surface and subsequently their colloidal stability in salty environments. Such a striking difference in colloidal stability was already noted

DOI: 10.1021/acsphotonics.5b00301
ACS Photonics 2015, 2, 1209−1216

for multipolar dyes having different geometry and electronic distribution (i.e., dipolar and octupolar).[4] The present work offers a unique insight into the energetics of the organization at the interface and opens directions for further improving the colloidal stability of the NPs by engineering the structure of the dipolar dye (nature and length of the π-conjugated system, presence of side groups). In particular the lipophilic/hydrophilic balance and its distribution over the dipolar dye axis will be adjusted in order to further stabilize the polar order of dyes on the NPs' surface.

CONCLUSION

We have undertaken polarization-resolved SHS experiments to investigate a series of two FONs made from dipolar chromophores (push−pull type) bearing a triphenylamine-donating end-group and a slightly hydrophilic acceptor end-group. With the SHS method, we come up with a new and noninvasive method to characterize the structure of the NPs and their evolution and stability by following their multipolar response when adding salt.

We have characterized the quadratic nonlinear optical response (hyper-Rayleigh) of the constitutive dyes, which are relatively good NLO emitters. We have quantified the SHS signal of highly dispersed NPs (diameter ∼40 nm) made of these dyes using the reprecipitation method. The NPs are very bright SHS emitters (typically 6 orders of magnitude brighter than a dye), thus very attractive for single-particle tracking or bioimaging. A polar SHS plot exhibits two-lobe patterns that are typical of a dominant electric dipolar response attributed to a polar H-type aggregate arrangement at the water interface where the hydrophobic triphenylamine end-group points toward the center of the NP and the hydrophilic-like formyl end-group points toward water. For both NPs, when adding salt, four-lobe polar SHS plots are observed, indicating a strong decrease of the dipolar contribution against the octupolar one inside the previously dominant electric dipolar (local) response and an almost residual but constant effective electric quadrupolar (nonlocal) response probably coming from the NP bulk. We have thus quantified the decrease of the SHS signal when adding salt with the goal to measure the colloidal stability of the FONs. We have proposed a simple equilibrium model to quantify that evolution, which fits nicely the SHS decrease of the intensity and also depolarization ratio. From the obtained equilibrium constant linked to these data, we have extracted a lower bound free energy for the two NPs, which are thermally accessible (2.7 and 4.5 kJ/M) and in good accordance with their respective stability. The present study will be extended to other FONS made from dipolar dyes in order to quantify, using polarization-resolved SHS spectroscopy, the stability of the FONs depending on the chemical structure of the dipolar dyes. This will help us to optimize dye building blocks in view of their use in bioimaging. As such, SHS provides a unique help in the bottom-up molecular engineering of FONS with adjusted colloidal properties.

EXPERIMENTAL AND THEORETICAL SECTION

Dyes and Organic Nanoparticle Preparation. Dyes **1** and **2** were prepared according to the literature-reported procedures.[5,6] Organic nanoparticles (ONPs) were prepared using the reprecipitation method[19] by dropwise addition of a 1 mM solution in THF of dye **1**, **2**, or PLGA in deionized water (1:99, v/v) under gentle magnetic stirring. A transparent solution is readily obtained after the addition is completed. Electron microscopy (TEM) attested the formation of spherical NPs for all samples with an estimated size of about 40 nm (Figure 1). TEM was carried out using a Hitachi H7650, with deposit of an aliquot of ONPs on a copper grid coated with a carbon membrane that was positively charged using the Glow discharge technique. A solution of uranyl acetate was used in a staining procedure to enhance the contrast.

Zeta potentials of ONPs were measured with the SZ-100Z Horiba instrument. Several measurements were realized for each sample according to a predefined operating procedure. In order to estimate the chemical and colloidal stabilities of ONPs of dyes **1** and **2**, absorption spectra were recorded over time using a Jasco V-670 spectrophotometer. Nanoparticles made of dye **2** exhibit high stability in pure water, with almost no evolution of NPs over time (Figure 1).

Molecular Incoherent HRS Characterizations. The experimental setup is configured in a 90° scattering geometry for HRS detection and has been fully detailed previously.[12] HRS measurements were performed with diluted solutions (with concentrations ranging from 5×10^{-5} to 10^{-6} M) in chloroform or acetonitrile (HPLC grade), which was the internal reference.[20]

For biphotonic excitation techniques, it is safe to check all states of polarization of the incident light since for example HRS TO-LO polar contributions may occur, even in isotropic media, when collecting the scattered light perpendicularly to the plane of incidence.[21] The incident elliptical polarization, denoted by the angle Ψ, is obtained by using a combination of a rotating half-wave plate ($\lambda/2$) and a fixed quarter-wave plate ($\lambda/4$). $\Psi = 0°$ (90°) corresponds to a linear horizontal (vertical) polarization [H (V)] and $\Psi = \pm 45°$ indicates a left/right circular polarization. In the local electric (LE) dipolar response and considering a multipolar description,[9] which is worth detailing again here, the total incoherent harmonic scattered light for a binary solution (solvent (S)/chromophore (X)) in the diluted regime (with no absorption) is given by

$$I_{\psi V}^{2\omega} = G[\{C_S[|\beta|^2 C_{\Psi V}^{\mathrm{Incoh}}]_S\} + C_X[|\beta|^2 C_{\Psi V}^{\mathrm{Incoh}}]_X][I^{\omega}]^2 \quad \text{(E1)}$$

where

$$C_{\Psi V}^{\mathrm{Incoh}}(i) = \cos^4(\Psi) + \Delta^{\mathrm{LE}}(i)\cos^2(\Psi)\sin^2(\Psi) + \mathrm{DR}(i)\sin^4(\Psi) \quad \text{(E2)}$$

$$|\beta(i)|^2 = |\beta_{J=1}(i)|^2(1/45 + 4/105\rho^2(i)) \quad \text{(E3)}$$

G is a global constant containing geometrical, optical, and electrical factors of the experimental setup; C is the concentration (molarity) of the solvent or solute; $C_{\Psi V}^{\mathrm{Incoh}}$ is the orientational average of the molecular spherical components of the hyperpolarizability of the solvent or solute. The nonlinear anisotropy $\rho = |\beta_{J=3}/\beta_{J=1}|$ measures the relative contributions of the octupolar ($\beta_{J=3}$) and dipolar ($\beta_{J=1}$) components of the hyperpolarizability tensor. The parameter Δ^{LE} is given by $\Delta^{\mathrm{LE}}(i) = 2[-1 + (33/7)\rho^2(i)]/[1 + (12/7)\rho^2(i)]$ and the depolarization ratio $\mathrm{DR}(i) = I_{VV}/I_{HV} = 9[1 + (2/7)\rho^2(i)]/[1 + (12/7)\rho^2(i)]$ ranges between 3/2 (only octupolar contribution) and 9 (only dipolar contribution). These two parameters are not independent since they exactly fulfill the dipolar condition $\Delta^{\mathrm{LE}}(i) + \mathrm{DR}(i) = 7$. Finally, the total HRS intensity obtained without polarization analysis of the scattered beam is $\beta_{\mathrm{HRS}} = |\beta_{J=1}|[2(1/3 + \rho^2/7)/3]^{1/2}$.

DOI: 10.1021/acsphotonics.5b00301
ACS Photonics 2015, 2, 1209−1216

SHS Investigation of the Nanoparticles. SHS measurements of FONs were performed using ultradiluted solutions (with concentrations typically ranging from 10^{-10} to 10^{-11} M) in ultrapure water (milli-Q) containing 1% THF (SHS internal reference), which was previously calibrated with acetonitrile.

The intensity of light scattered by a system of many correlated molecules is not just a multiple of the scattering by a single molecule. We expect scattering with phase relation since the partial waves scattered by the various correlated molecules among each particle may interfere. This coherent-like contribution scales quadratically with the number of correlated molecules N.[22] Thus, the incoherent (self-molecular response) contribution becomes rapidly negligible versus the collective one as the size of the correlated volume or surface increases.

In that respect, the total harmonic scattered light for a binary solvent (S)/FONs (NPs) solution in the diluted regime (with no absorption at the harmonic frequency) is given by

$$I_{\psi V}^{2\omega} = G[\{C_S[|\beta|^2 C_{\Psi V}^{Incoh}]_S\} + C_{NPs}[|\beta|^2 C_{\Psi V}^{Coh}]_{NPs}][I^{\omega}]^2 \quad (E4)$$

The solvent contribution corresponds to a standard LE dipolar incoherent response described in the preceding section. In contrast, the individual NP contribution is a dynamical structure factor intrinsically coherent-like since it is composed of local electric dipole but also nonlocal electric dipole responses and local quadrupolar electric responses due to the finite size of the particles, which involves possible retardation effects at the fundamental and harmonic frequencies (Figure 6).[16]

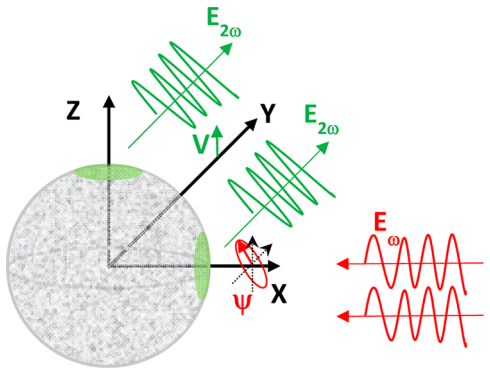

Figure 6. Sketch of the 90° scattering geometry for a spherical NP with vertical collection of the harmonic intensity $I_{\Psi V}^{2\omega}$. Due to the finite size of the NP, retardation effects at the fundamental and harmonic waves induce nonlocal electric dipole response and electric quadrupolar response, respectively.

In that respect we need to introduce the molar intensity response of each NP, $|\beta|^2 C_{\Psi V}^{Coh}$, where β stands for a hyperpolarizability and $C_{\Psi V}^{Coh}$ is a coherent-like polarization-dependent law similar to eq E2 given by

$$C_{\Psi V}^{Coh} = [\cos^4 \Psi + \Delta^{Coh} \cos^2 \Psi \sin^2 \Psi + DR \sin^4 \Psi] \quad (E5)$$

The depolarization ratio, $DR = I_{VV}/I_{HV}$, which concerns the linear state of incident and harmonic fields, should be dependent on the LE dipolar contribution; that is, it is expected to range still between the two limiting values 3/2 (octupolar beta component) and 9 (dipolar beta component) evoked previously. From eqs E4 and E5, when $\psi = 90°$, which corresponds to a vertical linear polarization for the fundamental wave, we observe that

$$I_{VV}^{2\omega} \propto DR \quad (E6)$$

This (simple) relation is very important because monitoring that polarized SHS intensity or extracting the depolarization ratio from polarization measurements is formally equivalent. This point is experimentally quite useful since it can be in some cases very difficult to measure the NPs' SHS parameters, for example, in the case of strong colloidal instabilities.

Finally, it is interesting to introduce the nonlocal dipolar and quadrupolar contributions as a unique effective quadrupolar contribution $\Delta^{Q_{eff}}$ defined by

$$\Delta^{Q_{eff}} = \Delta^{LE} - \Delta^{Coh} = (7 - DR) - \Delta^{Coh} \quad (E7)$$

This effective contribution corresponds to the deviation from the LE dipolar response introduced previously in eq E2, where $\Delta^{LE} = 7 - DR$.

AUTHOR INFORMATION

Corresponding Author

*E-mail: vincent.rodriguez@u-bordeaux.fr.

Notes

The authors declare no competing financial interest.

ACKNOWLEDGMENTS

This work has been done in the frame of "the Investments for the Future" Programme IdEx Bordeaux, LAPHIA (ANR-10-IDEX-03-02). V.R. is grateful to CNRS and Région Aquitaine for funding supports. M.B.D. gratefully acknowledges the Conseil Régional d'Aquitaine for financial support (Chair of Excellence to M.B.D. and fellowship to J.D.). TEM microscopy was done in the Bordeaux Imaging Center (UMS 3420 CNRS, University of Bordeaux/Inserm US4). The help of Sabrina Lacomme is acknowledged.

REFERENCES

(1) Horn, D.; Rieger, J. Organic Nanoparticles in the Aqueous Phase—Theory, Experiment, and Use. *Angew. Chem., Int. Ed.* **2001**, *40*, 4330.

(2) Fery-Forgues, S. Fluorescent organic nanocrystals and non-doped nanoparticles for biological applications. *Nanoscale* **2013**, *5*, 8428. Patra, A.; Chandaluri, C. G.; Radhakrishnan, T. P. Optical materials based on molecular nanoparticles. *Nanoscale* **2012**, *4*, 343 and references therein..

(3) Ishow, E.; Brosseau, A.; Clavier, G.; Nakatani, K.; Tauc, P.; Fiorini-Debuisschert, C.; Neveu, S.; Sandre, O.; Leaustic, A. Multicolor Emission of Small Molecule-Based Amorphous Thin Films and Nanoparticles with a Single Excitation Wavelength. *Chem. Mater.* **2008**, *20*, 6597.

(4) Parthasarathy, V.; Fery-Forgues, S.; Campioli, E.; Recher, G.; Terenziani, F.; Blanchard-Desce, M. Dipolar versus Octupolar Triphenylamine-Based Fluorescent Organic Nanoparticles as Brilliant One- and Two-Photon Emitters for (Bio)imaging. *Small* **2011**, *7*, 3219.

(5) Genin, E.; Gao, Z. J. A.; Varela, Z. J. A.; Daniel, J.; Bsaibess, T.; Gosse, I.; Groc, L.; Cognet, L.; Blanchard-Desce, M. Hyper-bright" Near-Infrared Emitting Fluorescent Organic Nanoparticles for Single Particle Tracking. *Adv. Mater.* **2014**, *26*, 2258—2261.

(6) Amro, K.; Daniel, J.; Clermont, G.; Bsaibess, T.; Pucheault, M.; Genin, E.; Vaultier, M.; Blanchard-Desce, M. A new route towards fluorescent organic nanoparticles with red-shifted emission and increased colloidal stability. *Tetrahedron* **2014**, *70*, 1903.

DOI: 10.1021/acsphotonics.5b00301
ACS Photonics 2015, 2, 1209−1216

(7) Clays, K.; Persoons, A. Hyper-Rayleigh Scattering in Solution. *Phys. Rev. Lett.* **1991**, *66*, 2980.
(8) Das, P. K. Chemical Applications of Hyper-Rayleigh Scattering in Solution. *J. Phys. Chem. B* **2006**, *110*, 7621−76630.
(9) Rodriguez, V.; Grondin, J.; Adamietz, F.; Danten, Y. Local Structure in Ionic Liquids Investigated by Hyper-Rayleigh Scattering. *J. Phys. Chem. B* **2010**, *114*, 15057.
(10) Eisenthal, K. B. Second Harmonic Spectroscopy of Aqueous Nano- and Microparticle Interfaces. *Chem. Rev.* **2006**, *106*, 1462.
(11) El Harfouch, Y.; Benichou, E.; Bertorelle, F.; Russier-Antoine, I.; Jonin, C.; Lascoux, N.; Brevet, P.-F. *J. Phys. Chem. C* **2014**, *118*, 609 and references therein..
(12) Castet, F.; Blanchard-Desce, M.; Adamietz, F.; Poronik, Y. M.; Gryko, D. T.; Rodriguez, V. Experimental and Theoretical Investigation of the First-Order Hyperpolarizability of Octupolar Merocyanine Dyes. *ChemPhysChem* **2014**, *15*, 2575−2581.
(13) Willetts, A.; Rice, J. E.; Burland, D. M.; Shelton, D. P. Problems in the Comparison of Theoretical and Experimental Hyperpolarizabilities. *J. Chem. Phys.* **1992**, *97*, 7590−7599.
(14) Rodriguez, E. V.; de Araújo, C. B.; Brito-Silva, A. M.; Ivanenko, V. I.; Lipovskii, A. A. Hyper-Rayleigh scattering from $BaTiO_3$ and $PbTiO_3$ nanocrystals. *Chem. Phys. Lett.* **2009**, *467*, 335.
(15) Le Dantec, R.; Mugnier, Y.; Djanta, G.; Bonacina, L.; Extermann, J.; Badie, L.; Joulaud, C.; Gerrmann, M.; Rytz, D.; Wolf, J. P.; Galez, C. Ensemble and Individual Characterization of the Nonlinear Optical Properties of ZnO and BaTiO3 Nanocrystals. *J. Phys. Chem. C* **2011**, *115*, 15140.
(16) Russier-Antoine, I.; Benichou, E.; Bachelier, G.; Jonin, C.; Brevet, P. F. Multipolar Contributions of the Second Harmonic Generation from Silver and Gold Nanoparticles. *J. Phys. Chem. C* **2007**, *111*, 9044.
(17) Lis, D.; Backus, E. H. G.; Hunger, J.; Parekh, S. H.; Bonn, M. Liquid flow along a solid surface reversibly alters interfacial chemistry. *Science* **2014**, *344* (6188), 1138.
(18) Revillod, G.; Duboisset, J.; Russier-Antoine, I.; Benichou, E.; Bachelier, G.; Jonin, C.; Brevet, P. F. Multipolar Contributions to the Second Harmonic Response from Mixed DiA-SDS Molecular Aggregates. *J. Phys. Chem. C* **2008**, *112*, 2716.
(19) Masuhara, H.; Nakanishi, H.; Sasaki, K., Eds. In *Single Organic Nanoparticles*; Springer-Verlag, 2003.
(20) Castet, F.; Bogdan, E.; Plaquet, A.; Ducasse, L.; Champagne, B.; Rodriguez, V. Reference Molecules for Nonlinear Optics: a Joint Experimental and Theoretical Investigation. *J. Chem. Phys.* **2012**, *136*, 024506.
(21) Rodriguez, V. New Structural and Vibrational Opportunities Combining Hyper-Rayleigh/Hyper-Raman and Raman Scattering in Isotropic Materials. *J. Raman Spectrosc.* **2012**, *43*, 627−636.
(22) Andrews, D. L.; Allcock, P. In *Optical Harmonics in Molecular Systems: Quantum Electrodynamic Theory*; Wiley-VCH: Weinheim, Germany, 2002.

DOI: 10.1021/acsphotonics.5b00301
ACS Photonics 2015, 2, 1209−1216